

- W. Krätschmer, K. Fostiropoulos, D. R. Huffman, *Chem. Phys. Lett.* **170**, 167 (1990); W. Krätschmer *et al.*, *Nature* **347**, 354 (1990).
- H. W. Kroto, J. R. Heath, S. C. O'Brien, R. F. Curl, R. E. Smalley, *Nature* **318**, 162 (1985); R. F. Curl and R. E. Smalley, *Science* **242**, 1017 (1988).
- H. Ajie *et al.*, *J. Phys. Chem.* **94**, 8630 (1990).
- R. Taylor, J. P. Hare, A. K. Abdul-Sada, H. W. Kroto, *J. Chem. Soc. Chem. Commun.* **1990**, 1423 (1990).
- D. S. Bethune, G. Meijer, W. C. Tang, H. J. Rosen, *Chem. Phys. Lett.* **174**, 219 (1990).
- J. M. Hawkins *et al.*, *J. Org. Chem.* **55**, 6250 (1990).
- D. M. Cox *et al.*, *J. Am. Chem. Soc.*, in press.
- P.-M. Allemand *et al.*, *ibid.* **113**, 1050 (1991).
- R. D. Johnson *et al.*, *ibid.* **112**, 8983 (1990).
- R. J. Wilson *et al.*, *Nature* **348**, 621 (1990); J. L. Wragg *et al.*, *ibid.*, p. 623.
- R. Tycko *et al.*, *J. Phys. Chem.* **95**, 518 (1991).
- J. W. Arbogast *et al.*, *ibid.*, p. 11.
- P.-M. Allemand *et al.*, in preparation.
- R. E. Haufler *et al.*, *J. Phys. Chem.* **94**, 8634 (1990).
- P. W. Fowler, J. E. Cremona, J. I. Steer, *Theor. Chim. Acta* **73**, 1 (1988).
- R. L. Whetten *et al.*, *Mater. Res. Soc. Symp. Proc.*, in press.
- Details of the chromatographic separation: A total of 500 mg of carbon extract, adsorbed on 250 g of neutral alumina, activity I, was chromatographed on the same alumina using a flash chromatography column (dimensions 60 by 6.5 cm). Elution with hexane-toluene (95:5 v/v) without application of pressure gave pure C<sub>60</sub>. Gradually increasing the amount of toluene from 10% to 20% and finally 50% led to the isolation of C<sub>70</sub>. Flash chromatography initially with hexane-toluene (1:1, v/v) followed by mixtures with gradually higher toluene content, and finally pure toluene, afforded four yellowish mixed fractions (A to D). All four fractions were rechromatographed on neutral alumina columns (30 by 3 cm). Chromatography of fraction A with hexane-toluene (95:5 v/v) first led to the elution of residual C<sub>70</sub> followed by yellow solutions of highly enriched C<sub>76</sub> (Fig. 1b). The second fraction B was first chromatographed with hexane-toluene (95:5, v/v) to remove residual C<sub>70</sub> and C<sub>76</sub>. Increasing the amount of toluene to 7% led to the elution of C<sub>84</sub> contaminated with fullerenes of higher and lower masses. A second chromatography on alumina (20 by 2 cm) afforded solutions of highly enriched C<sub>84</sub> (Fig. 1c). The third fraction C was first chromatographed with hexane-toluene (85:15, v/v) to remove residual C<sub>76</sub> and C<sub>84</sub>. Increasing the toluene content in the eluant to 18% gave reddish solutions containing very pure C<sub>70</sub>O (Fig. 1d). Elution of fraction D with a toluene gradient (5 to 25%) in hexane led first to the isolation of residual C<sub>70</sub>, C<sub>76</sub>, and C<sub>84</sub> followed by solutions containing C<sub>90</sub> as the major product in addition to a lesser amount of C<sub>94</sub> (Fig. 1e). Further increase in the amount of toluene afforded highly enriched C<sub>94</sub> (Fig. 1f). The fullerenes C<sub>90</sub> and C<sub>94</sub> which were eluted with solvents of high toluene content contain C<sub>60</sub> and C<sub>70</sub> as minor contaminants (Figs. 1e and 1f). For solubility reasons, C<sub>60</sub> and C<sub>70</sub> show severe tailing during chromatography with solvents of low toluene content, and the tailing material is eluted with the toluene-rich solvents.
- Starting from 2.5 g of toluene-soluble soot extract, chromatography as described in (17) afforded 117 mg of a mixture of the higher fullerenes containing approximately 20% of residual C<sub>70</sub>, 40% of C<sub>76</sub>/C<sub>78</sub>, 10% of C<sub>84</sub>, 10% of C<sub>70</sub>O, 10% of C<sub>90</sub> and C<sub>94</sub>, and ≈10% of other fullerenes in the range between C<sub>70</sub> and C<sub>98</sub> as well as fullerene oxides and nitrides. From this mixture, a total of 12 mg of C<sub>76</sub>, 2 mg of C<sub>84</sub> and 2 mg of C<sub>70</sub>O was isolated in pure form. The remainder of these compounds was obtained as mixed fractions.
- F. Diederich *et al.*, *Science* **245**, 1088 (1989); K. E. Schriver, thesis, University of California, Los Angeles (1990). Both ArF (193 nm) and Nd:YAG/4 (266 nm) lasers have been used under low-fluence conditions (1 to 10 mJ cm<sup>-2</sup>) to simultaneously evaporate and ionize solid films of the various fractions under He-jet atmosphere into a reflectron-type time-of-flight mass spectrometer.
- E. A. Rohlfing, D. M. Cox, A. Kaldor, *J. Chem. Phys.* **81**, 3322 (1984); P. P. Radi *et al.*, *Chem. Phys. Lett.* **174**, 223 (1990).
- H. So and C. L. Wilkins, *J. Phys. Chem.* **93**, 1184 (1989); Y. Rubin *et al.*, *J. Am. Chem. Soc.* **113**, 495 (1991).
- <sup>13</sup>C NMR of C<sub>76</sub>: δ 135.75, 142.05, 142.13, 142.87, 142.92, 143.65, 144.10, 144.20, 145.95, 146.63, 146.71, 147.28, 149.27, 150.10, 152.76, 153.17.
- FAB mass spectra show that small amounts of the fullerene monoxides C<sub>76</sub>O (*m/z* = 928), C<sub>84</sub>O (*m/z* = 1024), C<sub>90</sub>O (*m/z* = 1096), and of the dioxide C<sub>70</sub>O<sub>2</sub> (*m/z* = 872), which were not isolated, are also formed during the resistive heating process. The formation of the trioxides C<sub>72</sub>O<sub>3</sub>, C<sub>80</sub>O<sub>3</sub>, C<sub>86</sub>O<sub>3</sub>, and C<sub>90</sub>O<sub>3</sub>, which would give the same molecular ions at unit mass resolution than the higher fullerenes C<sub>76</sub>, C<sub>84</sub>, C<sub>90</sub>, and C<sub>94</sub>, respectively, is ruled out based on the observed fragmentation patterns. In addition to the fullerene monoxides, the FAB spectra suggest the formation of the carbon nitrides C<sub>76</sub>N (*m/z* = 926), C<sub>84</sub>N (*m/z* = 1022), and C<sub>90</sub>N (*m/z* = 1094). The formation of the methylene derivatives C<sub>77</sub>H<sub>2</sub>, C<sub>85</sub>H<sub>2</sub>, and C<sub>91</sub>H<sub>2</sub>, which would show the same molecular ions at unit mass resolution, is less probable under the experimental conditions.
- E. Vogel, M. Biskup, W. Pretzer, W. A. Böll, *Angew. Chem. Int. Ed. Engl.* **3**, 642 (1964).
- H. A. Staab and F. Diederich, *Chem. Ber.* **116**, 3487 (1983).
- H. Kroto, *Pure Appl. Chem.* **62**, 407 (1990).
- Supported by the National Science Foundation (F.D., R.L.W., F.W.), the Office of Naval Research (F.D., R.L.W.), and a NATO fellowship (R.E.).

11 February 1991; accepted 8 March 1991

## Deep UV Photochemistry of Chemisorbed Monolayers: Patterned Coplanar Molecular Assemblies

CHARLES S. DULCEY, JACQUE H. GEORGER, JR., VICTOR KRAUTHAMER, DAVID A. STENGER, THOMAS L. FARE, JEFFREY M. CALVERT\*

Deep ultraviolet (UV) irradiation is shown to modify organosilane self-assembled monolayer (SAM) films by a photocleavage mechanism, which renders the surface amenable to further SAM modification. Patterned UV exposure creates alternating regions of intact SAM film and hydrophilic, reactive sites. The exposed regions can undergo a second chemisorption reaction to produce an assembly of SAMs in the same molecular plane with similar substrate attachment chemistry. The UV-patterned films are used as a template for selective buildup of fluorophores, metals, and biological cells.

**S**ELF-ASSEMBLED MONOLAYER (SAM) and multilayer films are of interest for both fundamental studies and technological applications. Such films can be used in thin-film optics, sensors and transducers, protective layers, high-resolution imaging materials, and functionalized surfaces with specific chemical, biological, or adhesive properties (1-4). SAM-forming materials may be physisorbed layers, such as Langmuir-Blodgett films, or chemisorbed layers, such as organothiols bonded to Au or organosilanes bonded to silica. Both types of SAM films inherently offer a high degree of control in the direction normal to the plane of the film and substrate. Chemisorbed films are more versatile and stable, because the interaction between the film precursor and the surface is much stronger than in physisorbed films (1). However, little work has been done to control the placement of mol-

ecules in the plane of the surface.

Two approaches for producing patterned chemisorbed SAM films have recently been reported. In one, selective surface coordination chemistry is used to bind different SAM precursors to a substrate with lithographically defined stripes of dissimilar metals (5). This approach lacks generality in that coplanar patterns of multiple SAMs with the same surface attachment chemistry cannot be produced on a substrate composed of a single material. Also, the assemblies produced by this technique are not coplanar because the metal steps are typically 20 times the SAM film thickness. Alternatively, conventional lithographic processing has been used to fabricate coplanar "orthogonal" SAMs (6). Patterns of a thick polymer photoresist are defined and used to block the chemisorption of a SAM film in selected areas of the substrate. After the photoresist has been stripped, the remaining substrate is modified with a second SAM film. This technique has significant drawbacks for the formation of molecular assemblies, particularly the necessity of at least 18 processing steps.

This report describes a new approach for directly modifying and patterning SAM films by exposure to deep UV radiation.

C. S. Dulcey and J. H. Georger, Jr., Geo-Centers, Inc., Fort Washington, MD 20744.

V. Krauthamer, U.S. Food and Drug Administration, Center for Devices and Radiological Health, Rockville, MD 20857.

D. A. Stenger, T. L. Fare, J. M. Calvert, Center for Bio/Molecular Science and Engineering, Code 6090, Naval Research Laboratory, Washington, DC 20375.

\*To whom correspondence should be addressed.

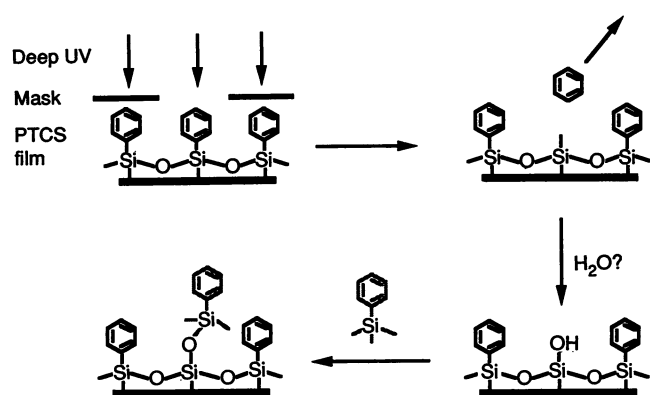


**Fig. 1.** Schematic of PTCS deep UV photochemistry and formation of a coplanar molecular assembly using the same SAM precursor. The second PTCS unit attaches to the exposed region of the original PTCS film.

Subsequent chemical treatments can produce coplanar molecular assemblies and selectively build up patterns of fluorophores, metals, and biological cells.

Organosilane films were prepared on glass and fused silica slides, Pt films on Si substrates, and Si wafers with a native oxide ( $\sim 15$  Å thick) or thermally grown oxide ( $\sim 350$  Å thick). Phenyltrichlorosilane (PTCS), benzyltrichlorosilane (BTCS), 3-aminopropyltrimethoxysilane (APTS), *N*-(2-aminoethyl-3-aminopropyl)trimethoxysilane (EDA), and (tridecafluoro-1,1,2,2-tetrahydrooctyl)-1-dimethylchlorosilane (13F) were used as the SAM film precursors. Chloro- and methoxysilanes react with hydroxyl groups on the surface of a substrate to form covalent siloxane (Si-O-Si) bonds and liberate HCl or methanol as reaction by-products (7). The film formation procedures were intended to produce homogeneous monolayer films and to avoid multilayer deposits (8, 9).

Using the sessile drop method (10), we found that water contact angles for the various cleaned substrates were typically  $10^\circ$  or less. After reaction with PTCS, BTCS, or 13F, the surfaces became hydrophobic, with contact angles ranging from  $58^\circ$  to  $65^\circ$  for PTCS,  $64^\circ$  to  $74^\circ$  for BTCS, and  $86^\circ$  to  $94^\circ$  for 13F. The variation of contact angle across a particular substrate was typically  $<5^\circ$ , indicative of homogeneous film coverage. The contact angle of the treated surfaces was not dependent on the substrate material. Reaction with APTS or EDA caused the contact angle to increase to only  $21^\circ$  to  $27^\circ$ , the result of polar primary amine terminal groups.

UV spectroscopy was used to characterize the aromatic silanes in solution and as SAM films on fused silica (11). The UV spectrum of PTCS in acetonitrile solution showed the spectrum of a benzene-like chromophore (12). The spectrum of PTCS on fused silica was similar but red-shifted by  $\sim 3$  nm relative to the solution spectrum. Replacement of the trichlorosilyl group with the siloxane linkages to the substrate thus has relatively little effect on the electronic structure and

absorption of this chromophore. EDA and APTS films showed a weak absorbance starting at 240 nm that increased gradually at shorter wavelengths. The 13F films showed no measurable absorbance at wavelengths greater than 190 nm.

We explored the deep UV photochemistry of PTCS and BTCS SAM films using pulsed krypton fluoride (248 nm) and argon fluoride (193 nm) excimer lasers as exposure sources. Both materials absorb strongly at the ArF wavelength but approximately 100-fold less at the KrF wavelength. Irradiation of a PTCS film at 193 nm caused a decrease in intensity of the entire spectrum. After irradiation at a dosage of  $400 \text{ mJ/cm}^2$ , the spectrum was reduced to baseline noise. A similar spectral change was obtained by irradiation at 248 nm, although the dosage required to reduce the spectrum to baseline noise was more than  $50 \text{ J/cm}^2$ .

The same photochemical changes were observed over a wide range of radiation intensity. Pulsed power densities used in these experiments ranged between 6 and  $600 \text{ kW/cm}^2$ . Equivalent results were obtained with high- and low-pressure Hg lamps, which have deep UV outputs that range from tens of milliwatts to several microwatts per square centimeter.

The wettability of a PTCS film on a glass slide increased with increasing exposure

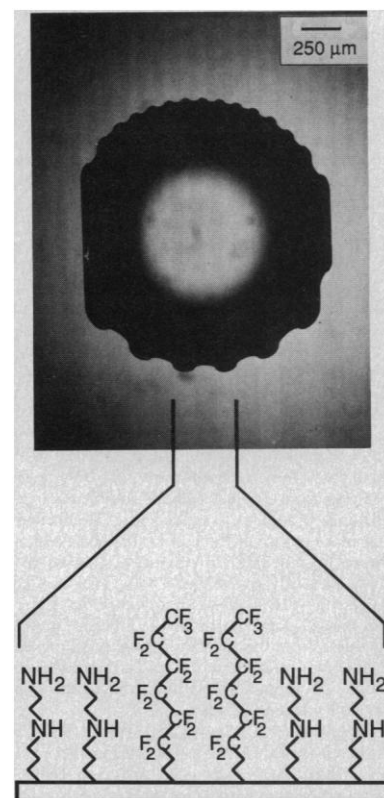
dose at 193 nm. The water contact angle decreased monotonically from  $58^\circ$  to below  $16^\circ$ , leveling off at  $\sim 400 \text{ mJ/cm}^2$ . The photochemical process directly correlates with the formation of polar, hydrophilic groups at the surface. UV spectroscopy of PTCS films irradiated at 193 nm under a blanket of  $\text{N}_2$  indicated that the same final photochemical result occurs in the presence or absence of  $\text{O}_2$ .

The spectroscopic and surface wettability changes described above for PTCS were also observed for BTCS films. Deep UV exposure of the PTCS film either caused the phenyl or benzyl chromophore to be removed from the film or photochemically altered the material to a species that had no absorption above 190 nm.

The efficiency of the organosilane photochemistry appears to depend on the nature of the underlying substrate. Approximately two to four times the dosage was required to effect the same change in surface wettability with a silicon native oxide or metal substrate as with silicon thermal oxide or glass substrates.

To identify the desorbed photoproducts resulting from deep UV irradiation, we investigated PTCS films on Si thermal oxide substrates, using Fourier transform mass spectrometry (FTMS) (13). After laser exposure, material desorbed from the surface is ionized, trapped, and mass-analyzed. The multiplex nature of FTMS is ideal for the study of monolayer systems, because an

**Fig. 2.** Wettability of patterned coplanar two-component SAM films. An EDA film was exposed to patterned 193-nm radiation ( $13 \text{ J/cm}^2$ ), followed by treatment with 13F. A water drop was placed on the patterned EDA/13F film and viewed by transmission optical microscopy. Darkening of the areas exposed to radiation was attributed to color center formation in the glass. The inward curvatures of the water drop on the dark stripes correspond to the exposed regions of the EDA film that were resilanized with 13F. The outward curvatures (light stripes) are due to spreading on the unirradiated, hydrophilic EDA film. The change in periodicity of the rippling follows the change in the line-space pairs of the mask as seen from the color centers. Molecular structures of the EDA and 13F films, and their location in the patterned assembly, are shown schematically below the drop.



entire mass spectrum can be obtained from the submonolayer quantity of material desorbed by a single laser pulse (14). Films of PTCS irradiated at both 193 and 248 nm yielded the same photoproduct, mass-to-charge ratio ( $m/z$ ) 78, corresponding to benzene. The generation of a fragment corresponding to  $C_6H_6$  instead of  $C_6H_5$  may result from H abstraction from a neighboring PTCS group in the film or by reactions in the plume of photodesorbed species near the surface. The signal-to-noise ratio of mass spectra at each wavelength was proportional to the corresponding absorption coefficients. No evidence for Si or organosilicon fragments was observed. Similar behavior has been observed for other aromatic silane SAMs.

To identify the surface-bound photoproduct, we exposed a BTCS film on a Pt substrate to 2 J/cm<sup>2</sup> at 193 nm, the dosage required to change the contact angle from 70° to <25°. The x-ray photoelectron spectroscopy (XPS) signals for Si showed no loss of intensity (15). XPS studies of other silane SAM films also showed that Si remained on the surface after irradiation.

The spectroscopic and wettability studies of the PTCS SAM films indicate that the organic chromophore is photodesorbed from the surface, the Si atom from the organosilane precursor remains bound to the surface after exposure, and the irradiated surface is highly wettable. These observations are consistent with a photochemical mechanism that involves cleavage at the Si-C bond to form a volatile (or removable) organic product and a polar siliceous species, likely a silanol (Si-OH).

It is not surprising that exposure of SAM films to deep UV radiation leads to bond breakage. The energy of a 193-nm photon (148 kcal/mol) is greater than any of the bond energies in the PTCS molecule (16, 17). However, photocleavage in the PTCS

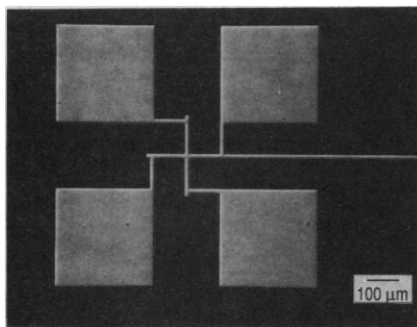


**Fig. 4.** Optical micrograph of a thin electroless Ni film (~600 Å) deposited on a patterned SAM film on Si thermal oxide. Film was exposed with a deep UV Hg lamp contact printer.

and BTCS SAM films apparently occurs only at the weakest link in the molecule, the Si-C bond (88 kcal/mol). The photochemical process does not appear to be ablative in nature, as it can be effected from sources ranging from low- and high-pressure Hg lamps to lasers. The laser powers generally used are below those typical of photoablation (18).

After cleavage of the Si-C bond, an extremely reactive Si atom (radical) would be left at the surface. Such a Si residue would react immediately outside an ultrahigh-vacuum environment with trace water to form silanol groups and yield the observed water-wettable, polar surface. As a direct consequence, these sites should be reactive to a variety of chemical coupling reactions, such as chemisorption of a second organosilane onto the photogenerated silanols. To demonstrate this, we irradiated a PTCS film on fused silica with 500 mJ/cm<sup>2</sup> of 193-nm light. The slide was then immersed in a toluene solution of PTCS under the same conditions as used in the initial film formation procedure. Both the contact angle and the UV spectrum of the slide after this

treatment were essentially the same as those of the original PTCS film. The patterned coplanar molecular assembly produced by UV irradiation and subsequent treatment with a solution of PTCS is shown in Fig. 1. The second PTCS SAM is attached to the remaining Si atom (or silanol) of the original SAM film.

Deep UV exposure of a SAM film followed by a second chemisorption reaction has also been used to produce coplanar molecular assemblies of different SAM materials with similar surface attachment chemistries. Flood exposure of an EDA film to 13 J/cm<sup>2</sup> of 193-nm radiation, followed by treatment of the substrate with a solution of 13F, produced a surface with a contact angle of about 90°, indicating that the perfluorinated silane had replaced the diamine in the irradiated areas. We repeated this experiment, using patterned deep UV radiation, to produce a two-component SAM film with alternating diamine and perfluoro functionalities. A micrograph of a water drop applied to the resulting surface is shown in Fig. 2. The scalloped edges of the water drop dramatically demonstrate the large differences in surface energy of adjacent sections of the film.

Patterned chemical reactivity or wettability properties of single or multicomponent SAM films can be used to build a variety of structures normal to the surface. For example, the reactivity of an aminosilane film was used as a template to produce a patterned monolayer of an organic fluorophore. An APTS film on fused silica was irradiated with patterned 193-nm light, then exposed to a solution of fluorescein isothiocyanate (FITC). FITC coupled via a thiourea linkage to the amine groups that remain in the unirradiated regions of the APTS film (Fig. 3).

Selective deposition of metal films has also been demonstrated by use of the deep UV

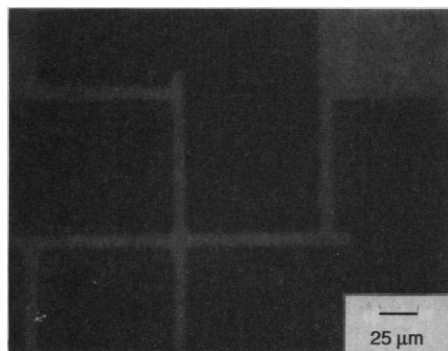


**Fig. 3.** Fluorescence micrograph of FITC coupled to a patterned APTS film. APTS on fused silica was irradiated with patterned 193-nm light (7.5 J/cm<sup>2</sup>) and then one side of the slide was exposed to ~5 mg of FITC in 250 ml of 1:1 dimethyl sulfoxide-bicarbonate buffer at pH 9.

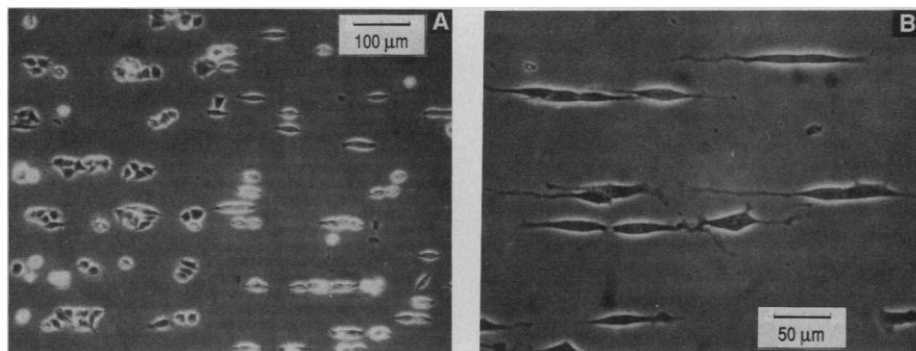


**Fig. 5.** Selective cell adhesion and outgrowth. Cells were plated at a density of  $8 \times 10^4$  cells/cm<sup>2</sup> on EDA/13F patterns, allowed 40 min to adhere, and gently rinsed with growth media. (A) Micrograph showing human SK-N-SH neuroblastoma cells at 10 min after rinsing. Note the elongation of cells on narrow EDA regions versus the spherical shape on wide regions (see text). (B) Neuroblastoma cells on narrow EDA/13F regions at 24 hours after rinsing. The outgrowth of neurites was confined to EDA regions.

patterning process. SAM films such as PTCS, BTCS, and APTS on Si substrates were exposed to either 193-nm or 248-nm radiation, then metallized with electroless plating techniques (19). Metal patterns typically several hundred angstroms thick were deposited only in the unexposed areas of the film (Fig. 4). These metal patterns can serve as plasma-hard etch barriers, conductive paths, or opaque regions for fabricating a wide variety of microelectronic devices.

Patterned two-component SAM films have also been used to produce arrays of more complex structures such as biological cells (6, 20). Coplanar EDA and 13F surfaces were plated with human SK-N-SH neuroblastoma cells (21) suspended in culture medium. On 40- $\mu\text{m}$ -wide EDA regions, the cells maintained relatively spherical shapes with visible contact points. However, with 12- $\mu\text{m}$  spacing, the widths of the alternating EDA/13F regions were less than the cell diameters, causing the cells to elongate to conform to the EDA lines (Fig. 5A). Subsequent neurite outgrowth after 24 hours was confined to the EDA regions (Fig. 5B).

The deep UV photochemistry of SAM films promises to be an interesting area of research and an enabling technology for manipulating molecular assemblies. SAMs are perhaps the ultimate materials for ultra-high-resolution imaging in optical and electron-beam lithographies (1, 2). Also, patterned adherent cells can facilitate advances in biosensors and implant devices. This process also provides a pathway to define patterns of molecular species such as chromophores, redox reagents, catalysts, and optically active and biologically active species at the practical limits of lateral resolution. The ability to photochemically control the wettability of a SAM film over a wide range of surface energy can provide insights into adhesion and biocompatibility at the molecular level. To reach these goals, it will be necessary to understand how the surface photochemical processes in SAM films depend on the type of substrate, the nature and energy of the exposure source, the surface attachment chemistry, and the specific chemical functionalities present in the SAM molecule.

#### REFERENCES AND NOTES

1. J. D. Swalen *et al.*, *Langmuir* **3**, 932 (1987).
2. G. G. Roberts, *Langmuir-Blodgett Films* (Plenum, New York, 1990), chap. 7.
3. G. M. Whitesides and P. E. Laibinis, *Langmuir* **6**, 87 (1990).
4. S. R. Wasserman, H. Biebuyck, G. M. Whitesides, *J. Mater. Res.* **4**, 886 (1989).
5. P. E. Laibinis, J. J. Hickman, M. S. Wrighton, G. M. Whitesides, *Science* **245**, 845 (1989).
6. D. Kleinfield, K. H. Kahler, P. E. Hockberger, *J. Neurosci.* **8**, 4098 (1988).
7. K. M. R. Kallury, U. J. Krull, M. Thompson, *Anal. Chem.* **60**, 169 (1988).
8. E. E. Polymeropoulos and J. Sagiv, *J. Chem. Phys.* **69**, 1836 (1978).
9. Substrates were cleaned by sequential 30-min immersions in 1:1 HCl/CH<sub>3</sub>OH and 18 M sulfuric acid, followed by multiple rinses with 18-megohm deionized water. The final rinse consisted of immersion in boiling deionized water. Residual water was removed from the substrates by immersions in acetone, followed by toluene. PTCS and BTCS films were formed by immersion of the substrates in a 1% (v/v) solution of the silane in anhydrous toluene for 3 to 5 min. The substrates were rinsed in toluene and baked at 120°C for 5 min. We prepared films of 13F by using the same procedure, except that the immersion time was 45 min. All chlorosilanes were handled under inert atmosphere conditions. We prepared films of APTS and EDA by transferring the substrates directly from the boiling water rinse to the deposition solution, which was 1% organosilane in 95% aqueous methanol with 10<sup>-3</sup> M acetic acid. After a 15-min immersion, the substrates were rinsed in anhydrous methanol and baked on a hot plate for 5 min at 120°C. Organosilanes were obtained from Huls Petrach Company (Bristol, PA). All cleaned and film-coated substrates were handled in a class 100 clean room.
10. W. Zisman, in *Contact Angles, Wettability and Adhesion*, vol. 43 of *Advances in Chemistry*, F. M. Fowkes, Ed. (American Chemical Society, Washington, DC, 1964), chap. 1.
11. The UV spectra were measured on a Cary 2400 spectrophotometer and were referenced to a clean, fused silica blank slide.
12. D. L. Doub and J. M. Vandenberg, *J. Am. Chem. Soc.* **69**, 2714 (1947).
13. FTMS experiments were performed in a Nicolet 3T superconducting magnet ion cyclotron resonance mass spectrometer. An apertured laser beam was passed through a Ni-mesh ion trap and focused onto the PTCS-coated substrate with estimated energy densities ranging from 2 to 20 mJ/cm<sup>2</sup>. Desorbed species were ionized by electron impact and mass-analyzed.
14. D. P. Land, C. L. Pettiette-Hall, D. Sander, R. T. McIver, J. C. Hemminger, *Rev. Sci. Instrum.* **61**, 1674 (1990).
15. We obtained XPS data by using an SSX-100-03 spectrometer (monochromatized Al K $\alpha$  source with a 600- $\mu\text{m}$  spot size and 45° takeoff angle).
16. R. Walsh, *Acc. Chem. Res.* **14**, 246 (1981).
17. S. W. Benson, *Thermochemical Kinetics* (Wiley, New York, 1976).
18. R. Srinivasan and B. Braren, *Chem. Rev.* **89**, 1303 (1989).
19. J. M. Schnur *et al.*, U.S. Patent Appl. 7,182,123, allowed.
20. D. A. Stenger, J. H. Georger, T. L. Fare, U. S. Patent Appl. 7,598,194, pending.
21. J. L. Biedler *et al.*, *Cancer Res.* **33**, 2643 (1973).
22. We acknowledge the assistance of M.-S. Chen and M. Anderson with SAM film preparation, S. McElvany and H. Nelson with the FTMS experiments, R. Colton with XPS experiments, and R. Binstead for UV spectroscopy software. Helpful discussions with G. Calabrese (Shipley Company) and J. Hickman (Science Applications International Corporation) are acknowledged. This work was supported in part by the MANTech office of the Assistant Secretary of the Navy, the Office of Naval Research, and the Office of Naval Technology.

5 December 1990; accepted 20 February 1991

## The *trk* Proto-Oncogene Product: A Signal Transducing Receptor for Nerve Growth Factor

DAVID R. KAPLAN, BARBARA L. HEMPSTEAD, DIONISIO MARTIN-ZANCA,\* MOSES V. CHAO, LUIS F. PARADA†

The *trk* proto-oncogene encodes a 140-kilodalton, membrane-spanning protein tyrosine kinase (p140<sup>prototr<sub>k</sub></sup>) that is expressed only in neural tissues. Nerve growth factor (NGF) stimulates phosphorylation of p140<sup>prototr<sub>k</sub></sup> in neural cell lines and in embryonic dorsal root ganglia. Affinity cross-linking and equilibrium binding experiments with <sup>125</sup>I-labeled NGF indicate that p140<sup>prototr<sub>k</sub></sup> binds NGF specifically in cultured cells with a dissociation constant of 10<sup>-9</sup> molar. The identification of p140<sup>prototr<sub>k</sub></sup> as an NGF receptor indicates that this protein participates in the primary signal transduction mechanism of NGF.

THE DEVELOPMENT OF THE VERTEBRATE nervous system is characterized by a series of complex events that

cause the apparently homogenous neuroepithelium of the early embryo to form the diverse, highly ordered, and interconnected neural cell types of the adult. Extensive evidence indicates that limiting diffusible factors are required for the targeting, survival, and proper synaptic arrangement of neurons (1). Neuronal circuits are sculpted from an initially overabundant production of neurons during development: In the midterm embryo, programmed cell death eliminates most of the neurons, leaving behind only those required for innervation of target tissues (2). Although neural adhesion and extracellular matrix molecules are essential for axonal migration, guidance, and growth cone targeting, most of the molecules that

D. R. Kaplan, Eukaryotic Signal Transduction Group, Advanced Biosciences Laboratory—Basic Research Program, National Cancer Institute—Frederick Cancer Research and Development Center, Frederick, MD 21702. B. Hempstead and M. Chao, Hematology-Oncology Division, Department of Medicine and Department of Cell Biology and Anatomy, Cornell University Medical College, New York, NY 10021. D. Martin-Zanca and L. F. Parada, Molecular Embryology Group, Advanced Biosciences Laboratory—Basic Research Program, National Cancer Institute—Frederick Cancer Research and Development Center, P.O. Box B, Frederick, MD 21702.

\*Present address: Instituto de Microbiología Bioquímica C. S. I. C., Universidad de Salamanca, 37008 Salamanca, Spain.

†To whom correspondence should be addressed.